Hybrid Lighting Enhances Color Accuracy in DLP-Based 3D Imaging

Erik M. Barrios[a,b], Jesus Pineda[a], Lenny A. Romero[c], María S. Millán[d], Andres G. Marrugo[a,*]
[a]Facultad de Ingeniería, Universidad Tecnológica de Bolívar, Cartagena, Colombia
[b]Esc. de Ciencias Básicas, Tecnología e Ingeniería, Universidad Nacional Abierta y a Distancia, Corozal, Colombia
[c]Facultad de Ciencias Básicas, Universidad Tecnológica de Bolívar, Cartagena, Colombia
[d]Dept. Óptica y Optometría, Universidad Politécnica de Cataluña, Terrassa, Spain

Abstract. Color accuracy is of immense importance in various fields, including biomedical applications, cosmetics, and multimedia. Achieving precise color measurements using diverse lighting sources is a persistent challenge. Recent advancements have resulted in the integration of LED-based Digital Light Processing (DLP) technology into many scanning devices for 3D imaging, often serving as the primary lighting source. However, such setups are susceptible to color-accuracy issues. Our study delves into DLP-based 3D imaging, specifically focusing on the use of hybrid lighting to enhance color accuracy. We presented an empirical dataset containing skin tone patches captured under various lighting conditions, including combinations and variations in indoor ambient light. A comprehensive qualitative and quantitative analysis of color differences (ΔE_{00}) across the dataset was performed. Our results support the integration of DLP technology with supplementary light sources to achieve optimal color correction outcomes, particularly in skin tone reproduction, which has significant implications for biomedical image analysis and other color-critical applications.

Keywords: Color accuracy, Digital Light Processing (DLP), light sources, 3D imaging, fringe projection profilometry.

*Andres G. Marrugo, agmarrugo@utb.edu.co

1 Introduction

Color accuracy is critical in many applications, including biomedical, cosmetic, and multimedia. It is particularly challenging in scenes with multiple or complex light sources. Often, the main light source in a three-dimensional (3D) scanning device is an LED-based digital light processing (DLP) projector,[1] which may introduce color-related problems such as chromatic aberration, spectral imbalance, and color temperature variation.[2] These factors can skew color representation and require further calibration for accurate imaging.

Color measurements depend strongly on the characteristics of the light source[3,4] and the optical properties of the subject matter.[5–7] These measurements may result in low color accuracy when

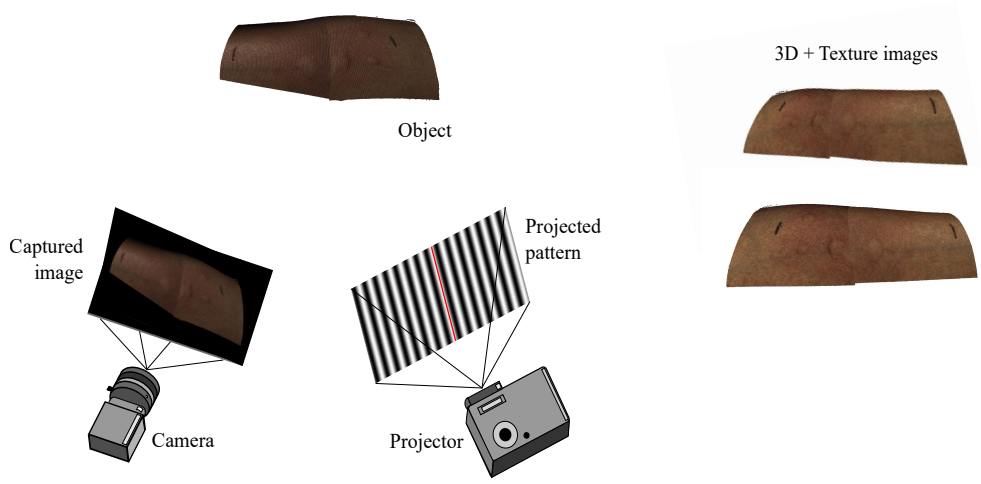

Fig 1 Fringe projection profilometry setup with a camera-projector pair. The color texture image is mapped onto the 3D surface topography. DLP projector lighting may introduce color accuracy problems in skin color measurements.

using DLP lighting in practical scenarios due to interactions with different light sources, such as indoor ambient light.[8,9] To overcome this problem, these complex lighting conditions require color correction techniques known as computational color constancy.[10,11] However, despite many advances in these techniques,[12,13] achieving high color accuracy in specialized applications such as medical imaging remains challenging.[14] For example, accurately reproducing skin color tones is difficult because of the interplay of light absorption, reflection, and scattering within the skin layers, demanding specialized calibration procedures.[6]

In many 3D imaging applications, the color texture image is simultaneously acquired along with the projected patterns for surface topography recovery.[15,16] For example, it is often obtained in Fringe Projection Profilometry (FPP) either by illuminating the surface of the object with uniform white light from the DLP projector or by projecting a black image to leverage ambient light (Fig 1). Moreover, the use of exclusive DLP lighting is often the choice in high-speed imaging.[17] In any case, the texture image may exhibit color accuracy problems.[18]

When applications require color for image analysis, like in skin imaging, ensuring accurate color measurements through a calibration procedure is crucial.[19,20] Tedla et al.[21] found that color calibration primarily fails because of lighting conditions, rather than the camera sensor. Their results showed that most consumer-grade sensors were suitable for color imaging under typical lighting environments but failed with narrowband lights like single-color LEDs. Hanlon et al.,[6] found that LED lighting is problematic for the visual separation of specific skin colors. Hence, LED-based DLP projectors, which use tri-color LEDs operated in sequence,[2] although designed for improved color accuracy may prove inadequate for skin color measurements. Furthermore, it remains unclear whether illuminating the scene solely with DLP light, environmental light, or a combination of the two is more effective.

In this study, we investigated the color accuracy of skin color tones across diverse lighting conditions in a DLP-based 3D measurement system. We used color patches carefully selected from a Munsell color checker chart to represent skin color tones. These patches were inspected under different illuminants simulating typical indoor lighting conditions and in combination with DLP lighting. This hybrid lighting approach successfully mitigates issues associated with color inaccuracies, offering a robust and practical framework for future research and applications in 3D imaging.

2 Materials and Methods

We analyzed the color accuracy related to the lighting effects in a DLP-based FPP 3D imaging system. We focused on skin color tones following a two-stage method. First, we selected a set of 23 color patches from the Munsell ColorChecker chart to represent a variety of skin colors, as well as different illuminants (DLP, D65, P15, and F) to simulate the interaction of the DLP light

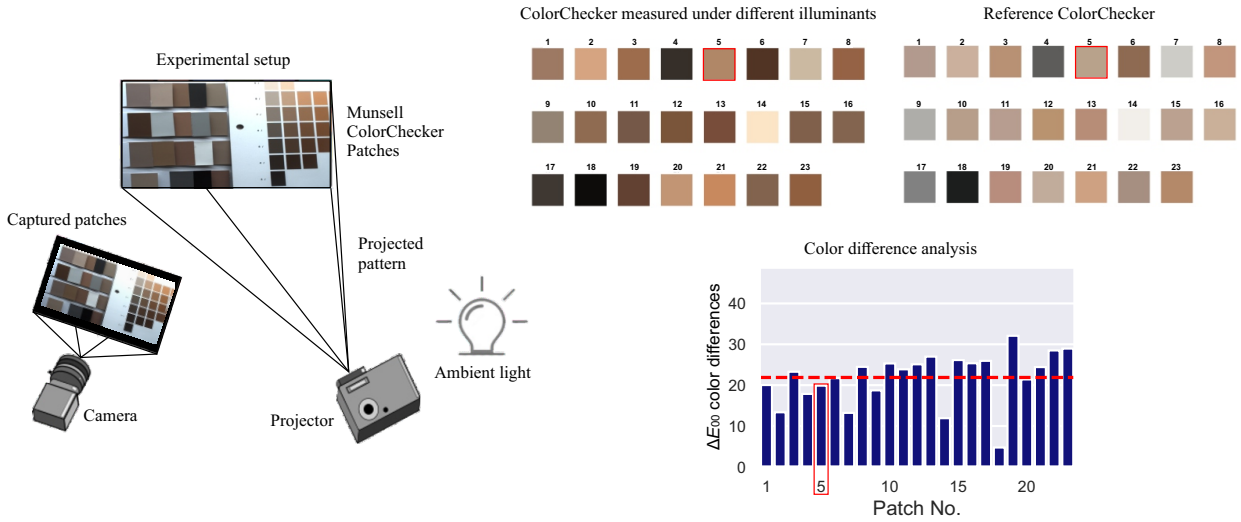

Fig 2 Methodology diagram for assessing color accuracy in a DLP-based Fringe Projection Profilometry (FPP) system under various lighting conditions. The selected skin tone color patches are compared to the reference values and the color differences are computed establish the most effective lighting configuration. Patch No. 5 was highlighted to illustrate the proposed methodology and the plot intepretation.

source with other typical light sources. Second, we performed the experimental acquisitions and colorimetric analysis of the different lighting conditions to determine the optimal lighting setup for precise skin color reconstructions in 3D imaging (Fig. 2).

2.1 Experimental Setup and Illumination Conditions

Our experimental setup consisted of a Basler acA1300-60gc GigE camera and a Dell M115HD DLP projector, configured in an observation booth[22] designed to evaluate color accuracy under various lighting conditions (Fig. 2). We used a combination of illuminants—D65 to represent average daylight (6500 K), P15 as a narrow-band phosphor fluorescent lamp (4100 K), and F as a tungsten filament lamp (2800 K)—to simulate typical indoor lighting[23] and their interactions with the DLP light source. In our experiments, we maintained a balance between the light source intensities to ensure consistent spectral shapes and stable chromatic results, highlighting the importance of balanced source intensities for obtaining reliable data. All radiometric, photometric and chromaticity specifications of the light sources are detailed in the publicly available repository. The

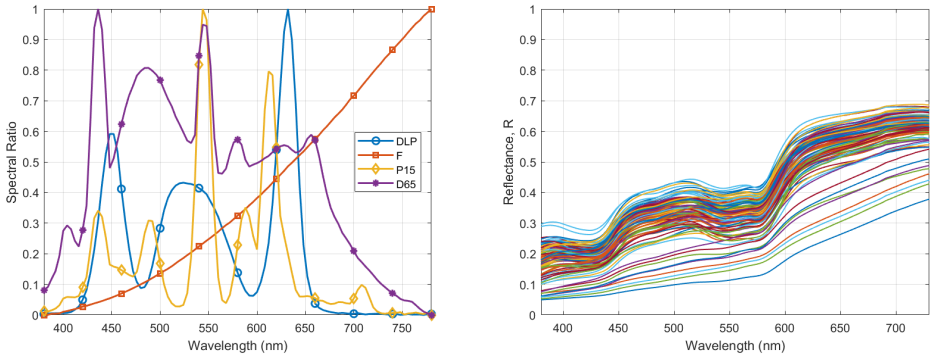

(a) (b)

Fig 3 Direct comparison of spectra and the impact of different illuminants on color accuracy, aiding in the design of a lighting scheme that optimizes color precision. (a) Normalized spectra of DLP, F, P15, and D65 illuminants. (b) Spectral reflectances of the 23 skin tone patches under D65 illumination.

setup was arranged to avoid specular reflections, ensuring consistent lighting for accurate color measurements.

In Fig. 3 (a) the normalized spectra of the DLP, P15, and F illuminants are presented for comparison. The DLP illuminant showed significant peaks between 450 and 650 nm, indicating a specific energy distribution at these wavelengths. The P15 illuminant has peaks that match the wavelengths of the DLP, although with a lower intensity, suggesting that P15 might complement the DLP by providing an additional energy distribution at the same wavelengths. However, illuminant F showed a constant upward trend with no significant peaks, indicating that it might not offer an energy distribution that matches the peaks of the DLP. This initial comparison suggests that P15 could potentially complement the spectrum of DLP better than illuminant F. Fig. 3 (b) shows the spectral reflectance of the ColorChecker skin tones under D65 illumination. This graph allows the visualization of how the D65 illuminant might affect color accuracy in skin tones, which is crucial for designing a lighting scheme that optimizes color accuracy in practical applications. The reflectance curves indicate that most skin tone patches exhibit higher reflectance values in the red region of the spectrum (600-700 nm) than in the blue and violet regions (400-500 nm). This

is expected given the natural spectral characteristics of skin tones. Additionally, darker skin tone patches tend to have lower and flatter reflectance curves across the spectrum, while lighter skin tones show more pronounced peaks, particularly in the red region.

2.2 Dataset acquisition and color calibration

To obtain representative skin colors, we used the NIST dataset comprising spectral information of human skin reflectance.[24] We used these reflectance data based on the D65 illuminant to calculate the sRGB components thereby enabling a uniform and reliable representation of different skin tones under standard lighting conditions. It is noteworthy that we used the D65 illuminant as our reference standard for all color-difference evaluations. From these sRGB components, we selected 23 representative skin color patches from the Munsell ColorChecker chart[25] for the color difference analysis[26] (Fig. 2). The color patches were captured under various illuminants: exclusively using a DLP projector (category I), combining DLP with other light sources (category II), and under lighting without DLP (category III), as detailed in Table 1.

To ensure that the color constancy is camera-independent, we applied a chromatic adaptation transform to the device-dependent RGB coordinates, transforming them to the sRGB standard.[27] This choice was made due to sRGB's widespread use and acceptance in visualization applications for human observers, facilitating result comparison and reproducibility. This was initially achieved by calculating the tristimulus values X, Y, and Z from the spectral data of the samples and illuminance. Subsequently, these values were converted to RGB values in the sRGB color space, considering specific corrections, such as gamma and linearization. The CAT02[28] color adaptation model was used to ensure color consistency in hybrid lighting conditions. The complete process is detailed in the publicly available repository. Most automatic white balance algorithms designed

Table 1 Illuminant combinations used in the experimental lighting scenarios.

Category	Lighting source	Abbreviation
I.	Only the digital light projector	DLP
II.	Digital light projector and D65 illuminant	DLP + D65
	Digital light projector and P15 illuminant	DLP + P15
	Digital light projector and F illuminant	DLP + F
	Digital light projector with D65 and P15 illuminants	DLP + D65 + P15
	Digital light projector with D65 and F illuminants	DLP + D65 + F
	Digital light projector with P15 and F illuminants	DLP + P15 + F
	Digital light projector with D65, P15, and F illuminants	DLP + D65 + P15 + F
III.	D65 illuminant	D65
	D65 illuminant with P15 illuminant	D65 + P15
	D65 illuminant with F illuminant	D65 + F
	P15 illuminant	P15
	P15 illuminant with F illuminant	P15 + F
	Illuminant F	F
	D65 illuminant, P15 illuminant, and F illuminant	D65 + P15 + F

on general statistical premises frequently fail in specialized scenarios where these assumptions do not hold.[29] Therefore, to ensure an accurate color representation, we disabled auto white balance.

2.3 Color differences

Upon completing the data acquisition with different lighting scenarios, we performed the colorimetric analysis by comparing the acquired data to the reference color values. We carried out the analysis by adopting the ΔE_{00} color difference metric.[30] The ΔE_{00} color difference was calculated by the CIEDE2000 formula given by,

$$\Delta E_{00} = \sqrt{\left(\frac{\Delta L^*}{k_L S_L}\right)^2 + \left(\frac{\Delta C'}{k_C S_C}\right)^2 + \left(\frac{\Delta H'}{k_H S_H}\right)^2 + R_T \left(\frac{\Delta C'}{k_C S_C}\right)\left(\frac{\Delta H'}{k_H S_H}\right)}, \tag{1}$$

where several factors are considered including chromatic differences ($\Delta C'$), hue difference ($\Delta H'$), weights for lightness (S_L), color (S_C), hue (S_H), and a rotation term (R_T). Additionally, the equation involves parametric factors k_L, k_C, and k_H, which can vary based on the experiment but are typically set to 1.

We computed the mean ΔE_{00} color difference values and their standard deviations for each

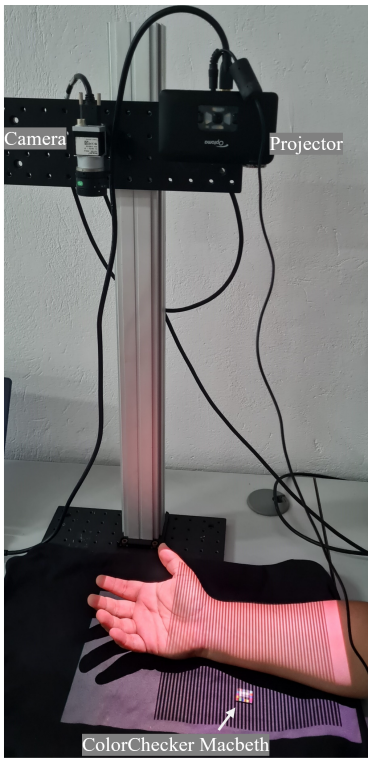

Fig 4 3D imaging setup composed of a camera, a projector and a Macbeth colorchecker.

lighting setup listed in Table 1 aiming to identify the most accurate and consistent conditions. Although the lowest mean ΔE_{00} value may indicate a specific optimal scenario, it is also important to consider lighting conditions with low variance for consistency. Finally, since often DLP lighting is unavoidable, we analyzed the best scenario that includes DLP lighting to establish best practices.

2.4 3D Reconstruction and calibration

For the 3D reconstruction process we calibrated the FPP setup following the technique proposed by Vargas et al.[31,32] This calibration ensured the accuracy and reliability of the 3D measurements obtained from the FPP setup. For the phase unwrapping, we employed a 3-step phase-shifting algorithm along with gray coding, which was acquired at a rate of 60 frames per second.[33] This approach allowed us to accurately extract the phase information from the deformed fringe patterns and generate a detailed depth map of the surface.

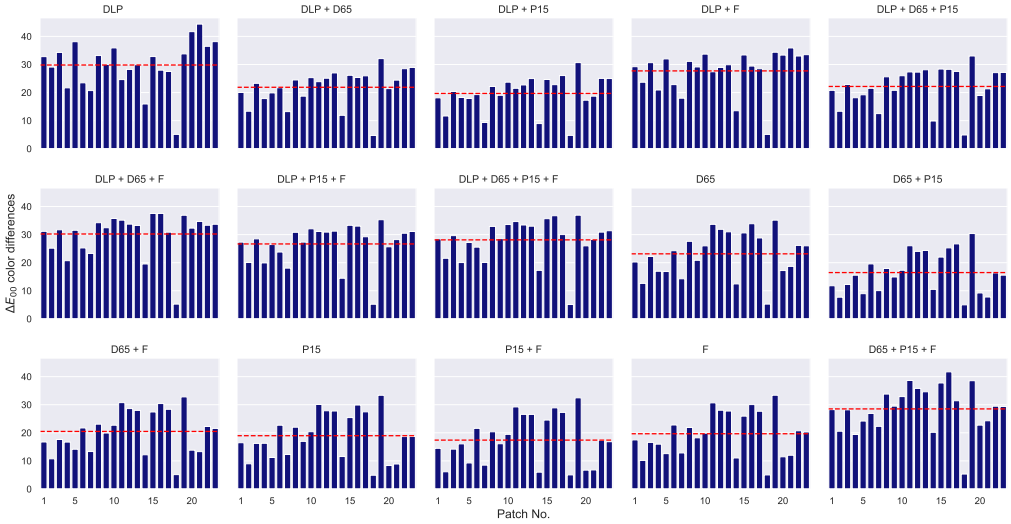

Fig 5 Comparative analysis of ΔE_{00} color differences under various lighting conditions.

To capture the texture image, we projected a white image using the DLP projector, which provided a uniform illumination across the skin surface. This allowed us to accurately capture the color and texture details of the skin. In scenarios where ambient illumination was used, a black image was projected to ensure that the DLP did not contribute to the illumination. In addition, we illustrate the experimental setup for 3D reconstruction in Fig. 4. This setup includes the integration of a camera, a DLP projector, and a Macbeth ColorChecker.

3 Results and discussion

The ΔE_{00} color differences across the 15 lighting configurations reveal significant variances in color accuracy for all 23 patches (Fig. 5). Notably, high color differences were obtained with the DLP as the exclusive light source. In contrast, lower color differences were obtained by combining the DLP with another light source, for example with the D65 and the P15 but not so much with the F. This discrepancy is indicative of the complex interplay between different light source characteristics and their impact on color accuracy. The P15 illuminant, with its narrow-band phosphor

Table 2 Mean and standard deviation values for the ΔE_{00} color differences from the 23 patches under the 15 lighting settings.

Lighting setup	Mean	Standard deviation
DLP	29.8154	8.7091
DLP + D65	21.8828	6.3518
DLP + P15	19.6937	6.1804
DLP + F	27.7143	7.4409
DLP + D65 + P15	22.1755	6.9020
DLP + D65 + F	30.2178	7.4658
DLP + P15 + F	26.6764	7.0491
DLP + D65 + P15 + F	28.1274	7.4231
D65	23.1549	8.0162
D65 + P15	16.4839	7.2055
D65 + F	20.4929	7.4768
P15	18.9729	8.0980
P15 + F	17.4033	8.6622
F	19.6691	7.7014
D65 + P15 + F	28.5148	8.1915

emission and moderate color temperature, complements the DLP's spectrum, enhancing overall color balance and reducing the ΔE_{00} values to more acceptable levels. Conversely, the F illuminant's broader spectral output at a lower color temperature appears less compatible with the DLP, failing to adequately correct the color differences probably due to the mismatched spectral outputs of the F illuminant's warm light and the DLP's cooler tones.

Our analysis in Fig. 5 highlights that patches with lighter skin tones (e.g., patches 19–23) consistently demonstrate higher ΔE_{00} values, indicating more pronounced color differences, especially under DLP lighting conditions. This sensitivity underscores their heightened reaction to spectral peaks in illuminants, posing significant challenges for achieving accurate color reproduction. Conversely, patches with darker skin tones exhibited lower ΔE_{00} values, suggesting reduced susceptibility to variations in the illuminant spectra owing to their broader wavelength absorption. This comparison underscores the distinct challenges involved in achieving precise color reproduction for lighter skin tones under DLP lighting conditions.

The average color differences, denoted with the red line in Fig. 5 and listed in Table 2, point to generally low color differences when two light sources are used but not necessarily when three are included. Moreover, the combinations of two light sources that do not include the DLP as a light source produce the lowest color differences (Table 2). These findings suggest that while DLP projectors can serve as a significant light source for color imaging, their spectral output may need to be carefully balanced with additional light sources to achieve optimal color accuracy. The results from the D65 and P15 combination imply that a mix of moderate and cooler temperatures in lighting can produce a more neutral white balance, which is conducive to lower color differences. However, the introduction of a third light source, particularly one with a warmer color temperature like the F illuminant, does not necessarily translate to improved color fidelity. Instead, it may introduce additional complexity to the color correction process, as seen in the increased average ΔE_{00} values. Our study highlights that combinations of light sources, particularly those incorporating a DLP projector, require precise spectral alignment to achieve optimal color accuracy. The pairing of DLP with P15 demonstrated a complementary spectral distribution, resulting in reduced ΔE_{00} values and enhanced color fidelity. However, the introduction of the F illuminant complicates this balance, because its spectral profile does not complement the DLP, resulting in elevated ΔE_{00} values. These findings underscore the importance of thoughtful design in multisource lighting setups to ensure spectral compatibility and mitigate challenges in color correction processes.

Given that our primary purpose was to focus on the DLP as a light source, we selected two distinct scenarios for a qualitative assessment by capturing the forearm of a subject (Fig 4). Case 1 used solely the DLP as a light source, and Case 2 the most consistent and favorable color correction configuration with the DLP+P15 light sources. These two cases are depicted in Fig. 6 with the color difference values, the RAW 3D color reconstruction, and the color-corrected 3D reconstructions.

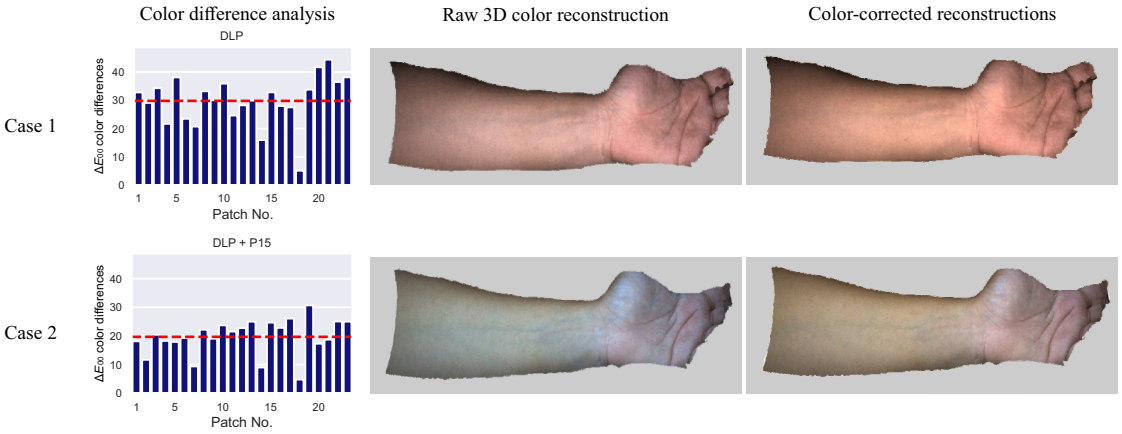

Fig 6 Two cases (one for each row) of 3D image reconstruction and color correction using DLP. For each case, from left to right, the first image represents the color difference analysis, the second displays the raw 3D color reconstruction, and the third exhibits color-corrected reconstructions.

The color-corrected output from Case 1 tends towards a warm or reddish tint obscuring finer details like vein patterns, which should be more pronounced. On the other hand, the output from Case 2 demonstrates a marked improvement: the skin tones are more natural, and the subtle variations, such as those around the palm and veins, are distinctly visible. These differences are also noticeable in the Color Checker images for the two cases depicting a closer appearance from the DLP+P15 to the reference values than the DLP (Fig. 7). The improved color differentiation in DLP+P15 suggests a more accurate representation of the subject's natural skin tones and thus improved color accuracy.

4 Conclusion

This study underscores the limitations of using Digital Light Processing (DLP) as a standalone light source for accurate color reproduction in 3D imaging. Our results reveal that a hybrid approach, specifically integrating DLP with the P15 illuminant, substantially improves color accuracy, especially in the context of skin tone reproduction. These findings have significant implications for medical image analysis, optical metrology, and other color-critical applications. Future research

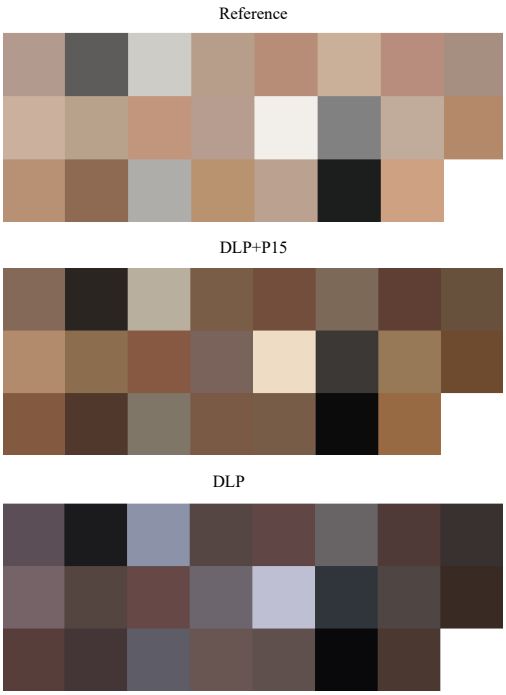

Fig 7 Exploring ColorChecker images and ΔE_{00} Reference vs. Lowest (Case 1) and optimal (Case 2) lighting conditions.

could focus on optimizing color correction algorithms under mixed lighting conditions and exploring other effective illuminant combinations. Overall, our study advocates for a comprehensive approach that pairs DLP with supplemental light sources for optimal color correction outcomes. For taking these results into the field, it may be useful to use simpler color constancy metrics such as the color inconsistency index (CII) instead of the ΔE_{00} metric for ease of use. However, further validation may be required.

Disclosures

The authors declare no conflicts of interest.

Code, Data, and Materials Availability

The authors confirm that all data underlying the findings are fully available without restriction. The final dataset and accompanying code are available on the following Open Science Framework

repository https://osf.io/m3xng/?view_only=5c5c9bcae8dc4b83a3179dc96884dce4 (the repository will be made public with DOI upon acceptance).

Acknowledgments

The authors acknowledge the financial support from the Universidad Technológica de Bolívar (project CI2021P04) and the Centre de Cooperació i Desenvolupament (CCD) at the Universitat Politècnica de Catalunya (project CCD 2020-B014). E. Barrios thanks Minciencias and Sistema General de Regalías (Programa de Becas de Excelencia) for a PhD scholarship.

References

1 A. G. Marrugo, F. Gao, and S. Zhang, "State-of-the-art active optical techniques for three-dimensional surface metrology: a review [invited]," *Journal of the Optical Society of America. A* **37**(9), B60–B77 (2020).

2 H. Jiang, Z. Lin, Y. Li, *et al.*, "Projection optical engine design based on tri-color leds and digital light processing technology," *Applied Optics* **60**(23), 6971–6977 (2021).

3 R. Khan, Y. Yang, Q. Liu, *et al.*, "Deep image enhancement for ill light imaging," *JOSA A* **38**(6), 827–839 (2021).

4 D. Kalustova, V. Kornaga, A. Rybalochka, *et al.*, "Color temperature tunable rgbw cluster with optimize color rendering and efficacy," *Optical Engineering* **62**(4), 045102–045102 (2023).

5 S. Tanaka, A. Kakinuma, N. Kamijo, *et al.*, "Auto white balance method using a pigmentation separation technique for human skin color," *Optical Review* **24**(1), 17–26 (2017).

6 K. L. Hanlon, G. Wei, L. Correa-Selm, *et al.*, "Dermoscopy and skin imaging light sources: a comparison and review of spectral power distribution and color consistency," *Journal of Biomedical Optics* **27**(8), 080902–080902 (2022).

7 K. Xiao, J. M. Yates, F. Zardawi, *et al.*, "Characterising the variations in ethnic skin colours: a new calibrated data base for human skin," *Skin Research and Technology* **23**(1), 21–29 (2017).

8 M. Corbalan, M. S. Millan, and M. J. Yzuel, "Color measurement in standard CIELAB coordinates using a 3CCD camera: correction for the influence of the light source," *Optical Engineering* **39**(6), 1470–1476 (2000).

9 M. D. Fairchild, *Color appearance models*, John Wiley & Sons (2013).

10 A. Gijsenij, T. Gevers, and J. Van De Weijer, "Computational color constancy: Survey and experiments," *IEEE transactions on image processing* **20**(9), 2475–2489 (2011).

11 J. Yang, M. Cai, and Z. Zhou, "Evolving convolution neural network by optimal regularization random vector functional link for computational color constancy," *Optical Engineering* **61**(10), 103102–103102 (2022).

12 V. Agarwal, B. R. Abidi, A. Koschan, *et al.*, "An overview of color constancy algorithms," *Journal of Pattern Recognition Research* **1**(1), 42–54 (2006).

13 D. H. Foster, "Color constancy," *Vision Research* **51**(7), 674–700 (2011).

14 D. Yung, K. Andy, R. T. Hsung, *et al.*, "Comparison of the colour accuracy of a single-lens reflex camera and a smartphone camera in a clinical context," *Journal of Dentistry* **137**, 104681 (2023).

15 J. Xu and S. Zhang, "Status, challenges, and future perspectives of fringe projection profilometry," *Optics and Lasers in Engineering* **135**, 106193 (2020).

16 J. Pineda, R. Vargas, L. A. Romero, *et al.*, "Robust automated reading of the skin prick test via 3d imaging and parametric surface fitting," *PloS one* **14**(10), e0223623 (2019).

17 S. Han, I. Sato, T. Okabe, *et al.*, "Fast spectral reflectance recovery using dlp projector," *International Journal of Computer Vision* **110**, 172–184 (2014).

18 S. Voisin, D. L. Page, S. Foufou, *et al.*, "Color influence on accuracy of 3d scanners based on structured light," *Proc. SPIE* **6070**, 72–80 (2006).

19 H. Takiwaki, L. Overgaard, and J. Serup, "Comparison of narrow-band reflectance spectrophotometric and tristimulus colorimetric measurements of skin color: Twenty-three anatomical sites evaluated by the dermaspectrometer® and the chroma meter cr-200®," *Skin Pharmacology and Physiology* **7**(4), 217–225 (1994).

20 A. R. Matias, M. Ferreira, P. Costa, *et al.*, "Skin colour, skin redness and melanin biometric measurements: comparison study between antera® 3d, mexameter® and colorimeter®," *Skin Research and Technology* **21**(3), 346–362 (2015).

21 S. Tedla, Y. Wang, M. Patel, *et al.*, "Analyzing color imaging failure on consumer-grade cameras," *JOSA A* **39**(6), B21–B27 (2022).

22 W. Chen, Z. Huang, Q. Liu, *et al.*, "Evaluating the color preference of lighting: the light booth matters," *Optics Express* **28**(10), 14874–14883 (2020).

23 R. Roa, R. Huertas, M. A. López-Álvarez, *et al.*, "A comparison between illuminants and light-source simulators," *Optica Pura y Aplicada* **41**(3), 291–300 (2008).

24 C. C. Cooksey, D. W. Allen, and B. K. Tsai, "Reference data set of human skin reflectance," *J. Res. Nat. Inst. Standards Technol.* **122**, 1–5 (2017).

25 C. S. McCamy, H. Marcus, and J. G. Davidson, "A color-rendition chart," *J. App. Photog. Eng* **2**(3), 95–99 (1976).

26 E. Kirchner, C. van Wijk, H. van Beek, *et al.*, "Exploring the limits of color accuracy in technical photography," *Heritage Science* **9**(1), 1–13 (2021).

27 H. Wannous, Y. Lucas, S. Treuillet, *et al.*, "Improving color correction across camera and illumination changes by contextual sample selection," *Journal of Electronic Imaging* **21**(2), 023015 (2012).

28 M. Luo and R. Hunt, "The structure of the cie 1997 colour appearance model (ciecam97s)," *Color Research & Application: Endorsed by Inter-Society Color Council, The Colour Group (Great Britain), Canadian Society for Color, Color Science Association of Japan, Dutch Society for the Study of Color, The Swedish Colour Centre Foundation, Colour Society of Australia, Centre Français de la Couleur* **23**(3), 138–146 (1998).

29 X. Li, G. Hou, L. Tan, *et al.*, "A hybrid framework for underwater image enhancement," *IEEE Access* **8**, 197448–197462 (2020).

30 G. Sharma, W. Wu, and E. N. Dalal, "The ciede2000 color-difference formula: Implementation notes, supplementary test data, and mathematical observations," *Color Research and Application* **30**(1), 21–30 (2005).

31 R. Vargas, A. G. Marrugo, S. Zhang, *et al.*, "Hybrid calibration procedure for fringe projection profilometry based on stereo vision and polynomial fitting," *Applied Optics* **59**(13), D163–D169 (2020).

32 R. Vargas, L. A. Romero, S. Zhang, *et al.*, "Pixel-wise rational model for a structured light system," *Optics Letters* **48**(10), 2712–2715 (2023).

33 S. Zhang, "Absolute phase retrieval methods for digital fringe projection profilometry: A review," *Optics and Lasers in Engineering* **107**, 28–37 (2018).

List of Figures

List of Tables